

Article

Control Reference Parameter for Stance Assistance Using a Passive Controlled Ankle Foot Orthosis—A Preliminary Study

Dimas Adiputra ^{1,2,*}, Mohd Azizi Abdul Rahman ^{1,*}, Ubaidillah ^{3,4,*}, Saiful Amri Mazlan ¹, Nurhazimah Nazmi ¹, Muhammad Kashfi Shabdin ¹ , Jun Kobayashi ⁵ and Mohd Hatta Mohammed Ariff ¹

¹ Advanced Vehicle System Research Group, Universiti Teknologi Malaysia, 54100 Kuala Lumpur, Malaysia; amri.kl@utm.my (S.A.M.); nurhazimah2@live.utm.my (N.N.); dekishaf@gmail.com (M.K.S.); mohdhatta.kl@utm.my (M.H.M.A.)

² Department of Electrical Engineering, Institut Teknologi Telkom Surabaya, 60234 Surabaya, Indonesia

³ Department of Mechanical Engineering, Universitas Sebelas Maret, 57126 Surakarta, Indonesia

⁴ National Center for Sustainable Transportation Technology, 40132 Bandung, Indonesia

⁵ Faculty of Computer Science and Systems Engineering, Kyushu Institute of Technology, 804-8550 Kitakyushu, Japan; jkoba@ces.kyutech.ac.jp

* Correspondence: adimas@ittelkom-sby.ac.id (D.A.); azizi.kl@utm.my (M.A.A.R.); ubaidillah_ft@staff.uns.ac.id (U.)

† These authors contributed equally to this work.

Received: 18 September 2019; Accepted: 6 October 2019; Published: 18 October 2019



Featured Application: The control reference parameter suggested in this study is implemented in a Passive-Controlled Ankle Foot Orthosis (PICAFO) equipped with magnetorheological (MR) brake on its ankle joint. Previously, the PICAFO has been shown to successfully deal with foot drop by locking the foot ankle position during the swing phase. By adding functions such as stance assistance, the user can get more benefits when using the PICAFO.

Abstract: This paper aims to present a preliminary study of control reference parameters for stance assistance among different subjects and walking speeds using a passive-controlled ankle foot orthosis. Four young male able-bodied subjects with varying body mass indexes (23.842 ± 4.827) walked in three walking speeds of 1, 3, and 5 km/h. Two control references, average ankle torque (aMa), and ankle angular velocity ($\dot{\omega}$), which can be implemented using a magnetorheological brake, were measured. Regression analysis was conducted to identify suitable control references in the three different phases of the stance. The results showed that $\dot{\omega}$ has greater correlation (p) with body mass index and walking speed compared to aMa in the whole stance phase ($p1(\dot{\omega}) = 0.666 > p1(aMa) = 0.560$, $p2(\dot{\omega}) = 0.837 > p2(aMa) = 0.277$, and $p3(\dot{\omega}) = 0.839 > p3(aMa) = 0.369$). The estimation standard error (Se) of the aMa was found to be generally higher than of $\dot{\omega}$ ($Se1(aMa) = 2.251 > Se1(\dot{\omega}) = 0.786$, $Se2(aMa) = 1.236 > Se2(\dot{\omega}) = 0.231$, $Se3(aMa) = 0.696 < Se3(\dot{\omega}) = 0.755$). Future studies should perform $\dot{\omega}$ estimation based on body mass index and walking speed, as suggested by the higher correlation and lower standard error as compared to aMa. The number of subjects and walking speed scenarios should also be increased to reduce the standard error of control reference parameters estimation.

Keywords: control parameter reference; stance assistance; magnetorheological brake; body mass index; walking speed; ankle torque; ankle angular velocity

1. Introduction

Walking gait assistance is essential, especially for people with abnormal gaits such as a weak ankle, spasticity, or foot drop [1]. These symptoms are common in post-stroke patients doing rehabilitation. In such cases, therapists and ancillary devices such as Ankle Foot Orthosis (AFO) may be used in gait assistance [2]. The AFO is an L-shape brace that covers the lower limb from the foot to the calf [3]. Figure 1 illustrates the gait assistance for foot drop patient using AFO. The reduction of dorsiflexion (e.g., blue circle) resulted in unwanted plantarflexion, which may lead to abnormal gait [4] toe-dragging when walking [5]. The patient should avoid toe-dragging, as this disturbs walking stability and increases the probability of a fall [6]. Here, the stiffness of the AFO joint restricts the unwanted plantarflexion, which then prevents the foot drop symptom occurrence, thus increasing walking stability. Because of this function, the post-stroke patients with foot drop symptom are usually suggested to use AFO to address their gait abnormalities in rehabilitation [7].

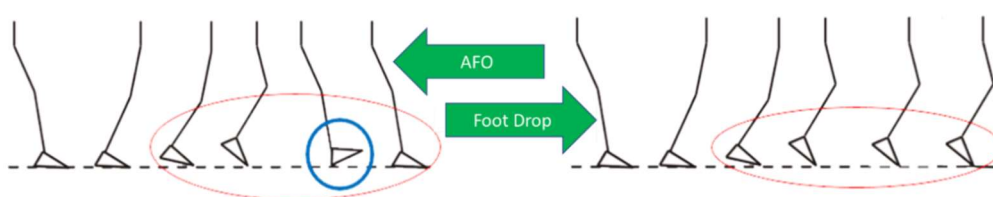


Figure 1. Illustration of foot drop treatment using Ankle Foot Orthosis (AFO).

The level of AFO restriction or AFO joint stiffness should be adjusted accordingly to achieve the maximum benefits [8]. For instance, sufficient work replacement by actuator will reduce muscle activity [9,10]. Different types of joints, such as rigid joint, flexible joint, and articulated joint, have different joint stiffnesses [11]. Rigid AFO has the highest possible joint stiffness, as the joint is fix and cannot rotate all. This AFO type is not suitable for treatment as it decreases the forward propulsion of the user by limiting the range of motion (ROM) [7,12]. A flexible AFO made from materials such as polypropylene [13] and carbon fiber [14] allows more ROM than a rigid AFO. However, the problem of a lack of forwarding propulsion remains [15]. Lastly, the articulated AFO allows maximum ROM as compared with the other two. It has electronic actuators (passive or active) and gait controller to control not only the joint stiffness but also ankle joint movement [11]. Therefore, an articulated AFO offers greater flexibility compared to rigid and flexible AFOs, and is capable of normal walking replication for intensive training purposes [16].

The previous study has developed a passive-controlled AFO (i.e., PICAFO in short). PICAFO is equipped with magnetorheological (MR) brake as a passive actuator for controlling the ankle joint stiffness using an electromyography (EMG) based Fuzzy Logic Controller (FLC) [17–19]. Surface electromyography or sEMG was used to classify the gait phases into two phases with a uniform threshold rather than a single threshold [20,21]. The two phases namely, Phase I runs from foot flat (FF) to heel off (HO), continuing to toe-off (TO), while phase II runs from TO to initial contact (IC) to FF. As shown in Figure 2, FLC also used additional information from ankle positions for controlling the MR brake stiffness. The result was that the controller could generate different joint stiffness in distinct gait phases [17], such as low and medium stiffness during the stance phase and high stiffness during the swing phase. The PICAFO successfully demonstrated foot drop prevention due to the high stiffness during the swing phase [18].

Despite that, the exact amount of joint stiffness, which was the control reference parameter, was pre-determined to be similar, even though different subjects and walking styles may require different joint stiffnesses during the stance and swing. Locking the ankle position during the swing phase could be done very straightforwardly by applying high stiffness, regardless of the subject and walking style [6]. However, the stiffness level during the stance phase, which prevents over dorsiflexion, was necessary to be adjusted accordingly [9]. Too much stiffness will distract the movement like rigid

and flexible AFO did, but insufficient stiffness will result in insignificant gait assistance [8]. Several research questions were highlighted as follows:

- (1) What is the suitable control reference parameter for stance assistance using PICAFO? Controlling the walking gait at the stance phase is not limited to the joint stiffness only. Other mechanical properties that can serve as the control reference parameter is also presented, such as motion parameter and assistive torque [11]. These mechanical properties are possible to be controlled using active actuators such as tracking and generation of the ankle motion path using electric motors [22–25], and assistive torque generation using pneumatics muscle [26–28] for balancing the body [29]. However, in this study, PICAFO was equipped only with MR brake as the actuator, which is not suitable for implementation of sophisticated control reference such as motion path. On the other hand, additional actuators are not a wise choice due to consideration of complex structure and overall weight of the PICAFO [30]. Because of that, mechanical properties such as ankle torque and ankle angular velocity were chosen to be investigated in this study since these can be controlled using an MR brake [31].
- (2) What critical parameter is suitable for estimation of the control reference parameter? Estimating the desired control reference requires information such as ground terrains, walking styles, user's anthropometrics, and other factors. In the previous study on AFO with MR brake, the control reference estimation which associated with the walking style such as the walking speed has been reported [32,33]. However, without investigation on the effect of the user's anthropometric such as body mass index (BMI) to the control reference. BMI is commonly used to describe human identity [34]. Thus, an additional critical parameter such as the BMI is expected to increase the control reference estimation accuracy.

To sum up, this preliminary study investigates the control reference parameters for stance assistance using PICAFO. The chosen control reference parameters were ankle torque and ankle angular velocity. On the other hand, the chosen critical parameters were walking speed and BMI. Section 2 further discussed the research materials and methods. Meanwhile, Sections 3 and 4 discussed the research findings and analysis, respectively.

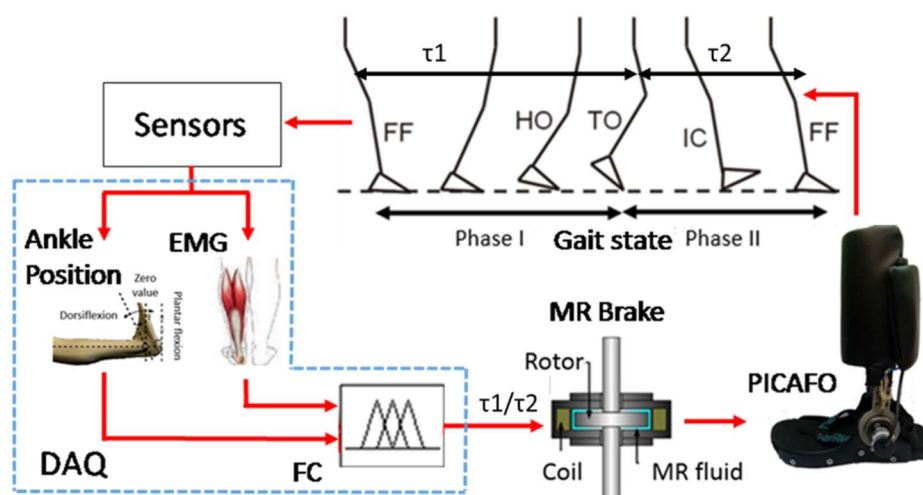


Figure 2. Passive-controlled AFO (PICAFO) system with fix ankle joint stiffness reference in distinct gait phases.

2. Materials and Methods

A walking experiment was conducted to answer the research questions. An advanced vehicle research group experiment was conducted in a rehabilitation engineering facility under Malaysia-Japan International Institute of Technology, Universiti Teknologi Malaysia, Kuala Lumpur, Malaysia.

Meanwhile, orthopedic doctors' committee, Institutional Review Board of Education Hospital of Universitas Sebelas Maret, Indonesia declared that the walking experiment in this study is safe for work involving human subjects (approval letter: No. 893/UN27.49/TU/2018). Young male subjects who could walk normally and had never suffered from any spasticity or foot symptoms in their life participated in a walking experiment. The subjects gave their written consent before experimenting. This section presents further details on the data collection, data processing, and data analysis for the walking experiment.

2.1. Data Collection

Four young male able-bodied subjects with body mass indexes (BMI) of 18.026, 23.072, 24.509, and 29.761, respectively, participated in the walking experiment. The setup was as shown in Figure 3. Subjects who could walk normally were selected for the experiment and each had never suffered from any spasticity and foot symptoms. Table 1 shows the details of the subjects anthropometric. The experiment was done by having the subjects walked on a treadmill using the PICAFO as a test measurement device, as shown in Figure 4. There were three sensors on the test device, namely a force sensor, rotary encoder, and accelerometer. Data from the sensors were sent to a personal computer through the USB-6211 data acquisition for data logging. Note that there was no applied controller for the PICAFO stiffness; thus, it had zero stiffness for the whole data collection. For each subject, there were three sessions of walking. The treadmill applied different walking speed, for instance, speeds (Sp) of 1 km/h, 3 km/h, 5 km/h represent slow, medium, and fast walking velocity, respectively. In each session, data of 20 steps of walking were collected and repeated two times. Therefore, there were a total of 480 walking steps observations for analysis.

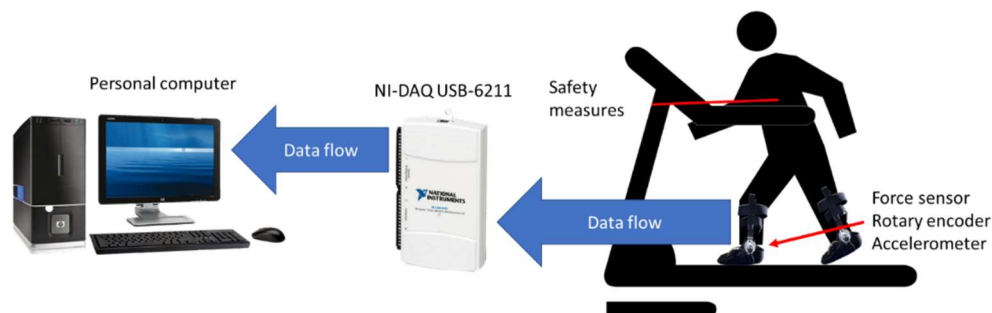


Figure 3. Experimental setup.

Table 1. Subject's anthropometric.

Anthropometric Parameters	Subject, Sb				Mean	Standard Deviation
	1	2	3	4		
Body mass (kg)	45	61.3	70	97.5	68.45	21.964
Height (m)	1.58	1.63	1.69	1.81	1.678	9.912
BMI	18.026	23.072	24.509	29.761	23.842	4.827
Gender	Male	Male	Male	Male	-	-
Age (year)	29	25	25	29	27	2.310
Foot mass (kg)	2.353	2.589	2.715	3.114	2.693	0.276
Foot length (m)	0.135	0.14	0.15	0.17	0.1488	0.0134

As illustrated in Figure 4, the sensor placement and walking steps data collected from the sensors are the followings:

1. Rotary encoder typed B1-106

Data collected: ankle position (θ), ankle angular velocity (ω), ankle angular acceleration (α).

Sensor placement: at the ankle joint right after the MR brake in the same axis. The standing position is the neutral position, dorsiflexion is a positive direction, and plantarflexion is a negative direction [17].

2. 3-axis accelerometer ADXL-335

Data collected: linear ankle acceleration (a).

Sensor placement: near the ankle joint with x-axis on the horizontal sagittal plane and y-axis on the vertical sagittal plane.

3. Force sensor FLX-A201

Data collected: ground reaction force on the heel (F_{heel}) and toe (F_{toe}).

Sensor placement: inside the PICAFO insole with fix position such as 9 cm of toe distance and 6 cm of heel distance from the ankle joint axis in the sagittal plane.

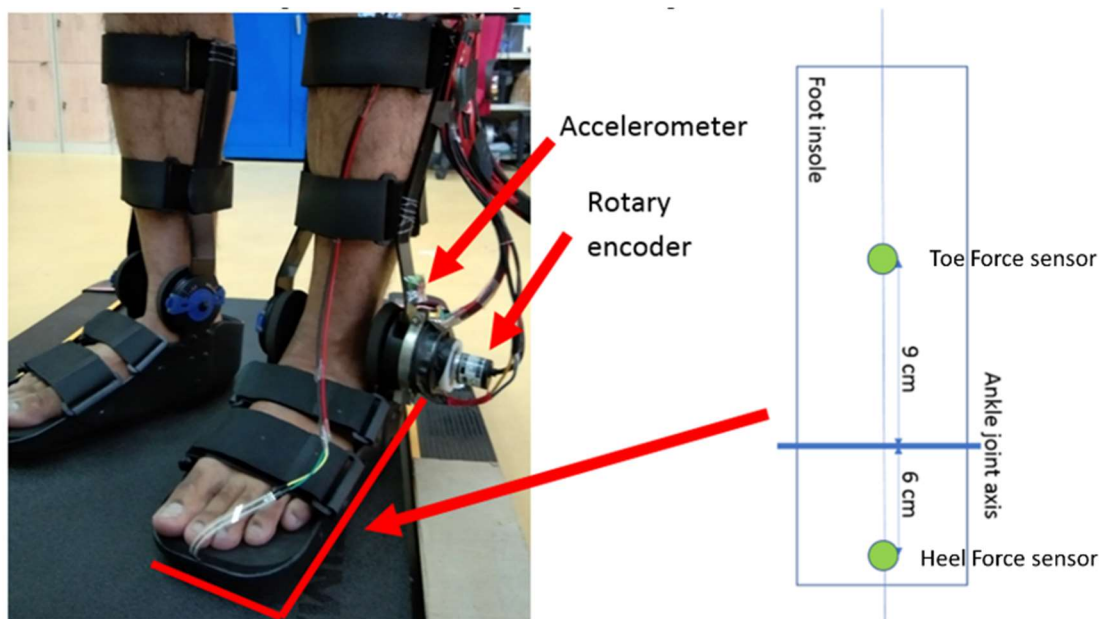


Figure 4. The PICAFO as testing device and sensors placement.

This research focused on the investigation of the ankle angular velocity and ankle torque. The ankle angular velocity could be measured directly from the rotary encoder. However, the ankle torque could not be measured directly. Therefore, the estimation of the ankle torque was conducted by using foot dynamic equations [35]. Free body diagram of a foot during walking is shown in Figure 5. Equations (1) and (2) described the net force equation on x-axis and y-axis. Equation (3) describes the net torque around the foot center of mass (CoM), in which F_a is the ankle force; M_a is the ankle torque; F_{toe} is the GRF on toe; F_{heel} is the GRF on heel; m is the foot mass; I is the foot inertia around the center of gyration (CoG); R is the distance of the working force to the CoM, g is the gravity constant; a is a linear acceleration of the ankle; and α is the angular acceleration of the ankle. The up, right, and counterclockwise (dorsiflexion) vectors are denoted with a positive (+ve) sign. Additionally, down, left, and clockwise (plantarflexion) vectors are denoted with a negative (-ve) sign.

$$F_{ax} + F_{toex} + F_{heelx} = ma_x \tag{1}$$

$$F_{ay} + F_{toey} + F_{heely} - mg = ma_y \tag{2}$$

$$M_a - F_a R_a + F_{toe} R_{toe} - F_{heel} R_{heel} = I\alpha \tag{3}$$

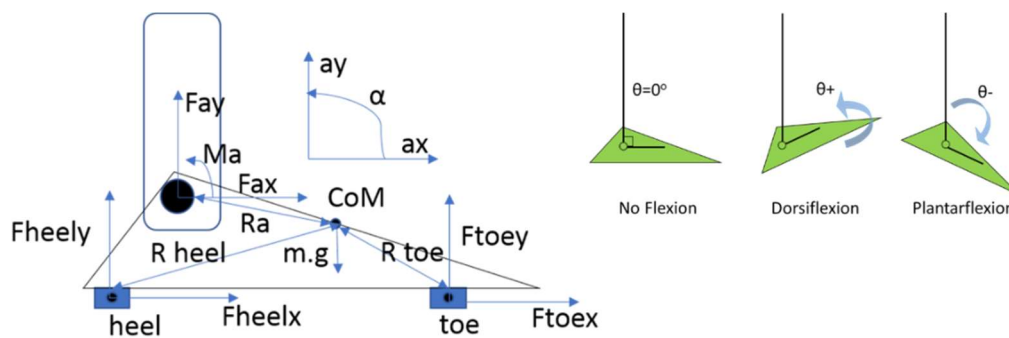


Figure 5. The foot dynamics.

Static and constant variables such as foot mass and foot length of the subject were measured before conducting the data collection. The foot mass was the total of the actual foot mass (1.45% of the body’s mass) and the PICAFO’s mass (1.7 kg) [35]. For example, subject 1 has a mass of 61.3 kg. Thus the foot mass for the dynamic calculation is $(61.3 \text{ Kg} \times 1.45\%) + 1.7 \text{ Kg} = 2.589 \text{ Kg}$. Foot mass and foot length were further used to determine the foot inertia (I), CoM, foot CoG, R_a , R_{toe} , and R_{heel} , as shown in Table 2. After all the necessary parameters were determined, the estimation of the ankle force could be done by solving Equations (1) and (2). Finally, the ankle force was included in Equation (3) for estimating the ankle torque M_a .

Table 2. The subject’s derived anthropometric.

Anthropometric Parameters	Subject, Sb				Mean	Standard Deviation
	1	2	3	4		
I ($\text{kgm}^2 \times 10^{-2}$)	0.967	1.144	1.378	2.030	1.380	0.403
CoG (m)	0.064	0.067	0.071	0.081	0.071	0.006
CoM, R_a (m)	0.068	0.070	0.075	0.085	0.074	0.067
R_{toe} (m)	0.028	0.018	0.015	0.015	0.019	0.005
R_{heel} (m)	0.122	0.132	0.135	0.135	0.131	0.005

2.2. Data Processing

In this research, the region of interest for investigating the control reference parameter was the stance phase only. In preventing foot drop, the PICAFO can generate a maximum stiffness to lock the foot position regardless of the subject’s anthropometric and walking style. Therefore, this study did not consider the swing phase for the investigation. Because of that, the collected data, such as the ankle torque and ankle angular velocity, were classified into three different phases of stance only such as IC to FF (1), FF to HO (2), and HO to TO (3). IC is when the foot contacts the ground on the heel first after the swing, while FF is when both toe and heel touch the ground while the body propelled forward. HO, as the name suggests, is when the heel is lifted, pushing the ground. TO starts when the foot begins to swing after being pushed off the ground. Measured data were divided into several phases to obtain the data average. The difference between the ankle position and the time-lapse defined the average ankle angular velocity ($a\omega$). On the other hand, the mean of all the data point presented in that phase defined the average ankle torque (aM_a). For illustration, see Figure 6.

2.3. Data Analysis

The goal of this preliminary research was to identify suitable control reference parameters ($a\omega$ or aM_a) for estimation based on BMI and walking speed (WS) in three different phases of stance. Regression analysis such as multiple R, R-squared, adjusted R-squared, the standard of error, and t-test for critical parameter coefficients were the tools. The regression error was assumed to be independent one to another with constant variance; thus, it has a normal distribution. Therefore, the regression response (control reference) and the slope parameter (critical parameter coefficient) were also normally

distributed. Table 3 presents the scenario for data analysis. The value of R explains the correlation between the critical parameter and control reference. A value for R near to one indicates better correlation. The standard error explains the relationship nature of the critical parameter and control reference. The less standard error means a better relationship. As for the t-test, it was conducted to see the probability of the critical parameter coefficient being zero (P -value > 0.05). Zero coefficient means that the critical parameter is insignificant for the control reference estimation.

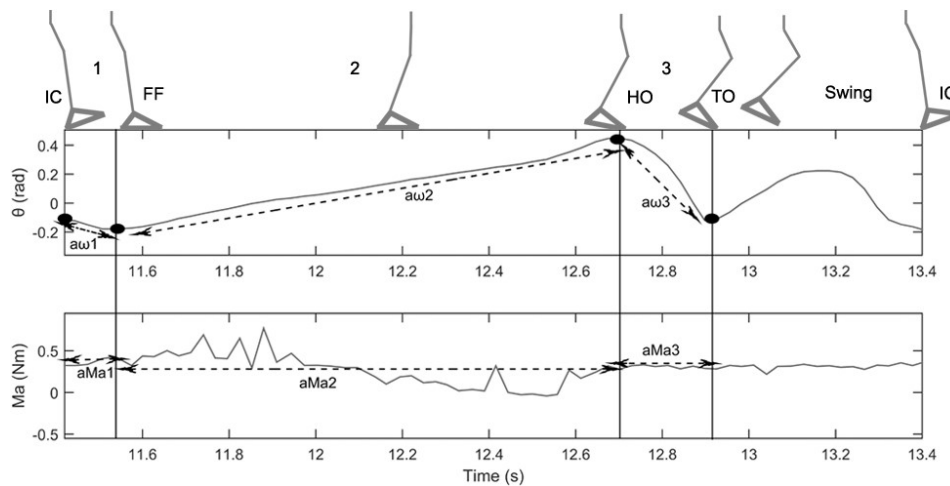


Figure 6. Average ankle torque and angular velocity in different stance phase (1, 2, 3).

Table 3. Data analysis scenario.

Case	Stance Phase	Critical Parameter		Control Reference	
		BMI	WS	$a\omega$	aM_a
1	IC to FF	✓		✓	
2		✓			✓
3			✓	✓	
4			✓	✓	✓
5			✓	✓	✓
6			✓	✓	✓
7	FF to HO	✓		✓	
8		✓			✓
9				✓	✓
10			✓	✓	✓
11			✓	✓	✓
12			✓	✓	✓
13	HO to TO	✓		✓	
14		✓			✓
15				✓	✓
16			✓	✓	✓
17			✓	✓	✓
18			✓	✓	✓

3. Result

This section describes the results of the data analysis. Figures 7–9 show the linear regression of control reference parameter $a\omega$ and aM_a during IC to FF, FF to HO, and HO to TO respectively. The estimation of the actual value (blue dot) was conducted based on walking speed (grey dash line) only; BMI (yellow dash line) only; and a combination of both (orange dotted line). The left graph shows the actual and estimated values from the walking speed point of view, while the right graph shows the actual and estimation value from the BMI point of view. Table 4 presents the regression statistic result. Lastly, Table 5 presents the estimation value and t -test results of the critical parameter coefficient for multiple regression of control reference parameter $a\omega$ and aM_a .

The correlation of the control reference parameter with walking speed shows an inverse relationship. If $a\omega$ has a positive correlation, then aM_a has a negative correlation (Figure 8) and vice versa (Figures 7 and 9). Meanwhile, from a BMI point of view, a similar correlation behavior is also observed, however with a less steep gradient. The analysis considered only the absolute correlation value. Table 4 presents the correlation analysis results in terms of multiple R (p), and R-squared (p^2). The results show that the combination of walking speed and BMI to the control reference parameter has the highest correlation score compare to when they are just a stand-alone critical parameter in all stance phases. This result is also consistent for both the control reference parameter $a\omega$ and aM_a . However, the highest correlation score belonged to $a\omega$ instead of aM_a ($p1(a\omega) = 0.666 > p1(aM_a) = 0.560$, $p2(a\omega) = 0.837 > p2(aM_a) = 0.277$, and $p3(a\omega) = 0.839 > p3(aM_a) = 0.369$).

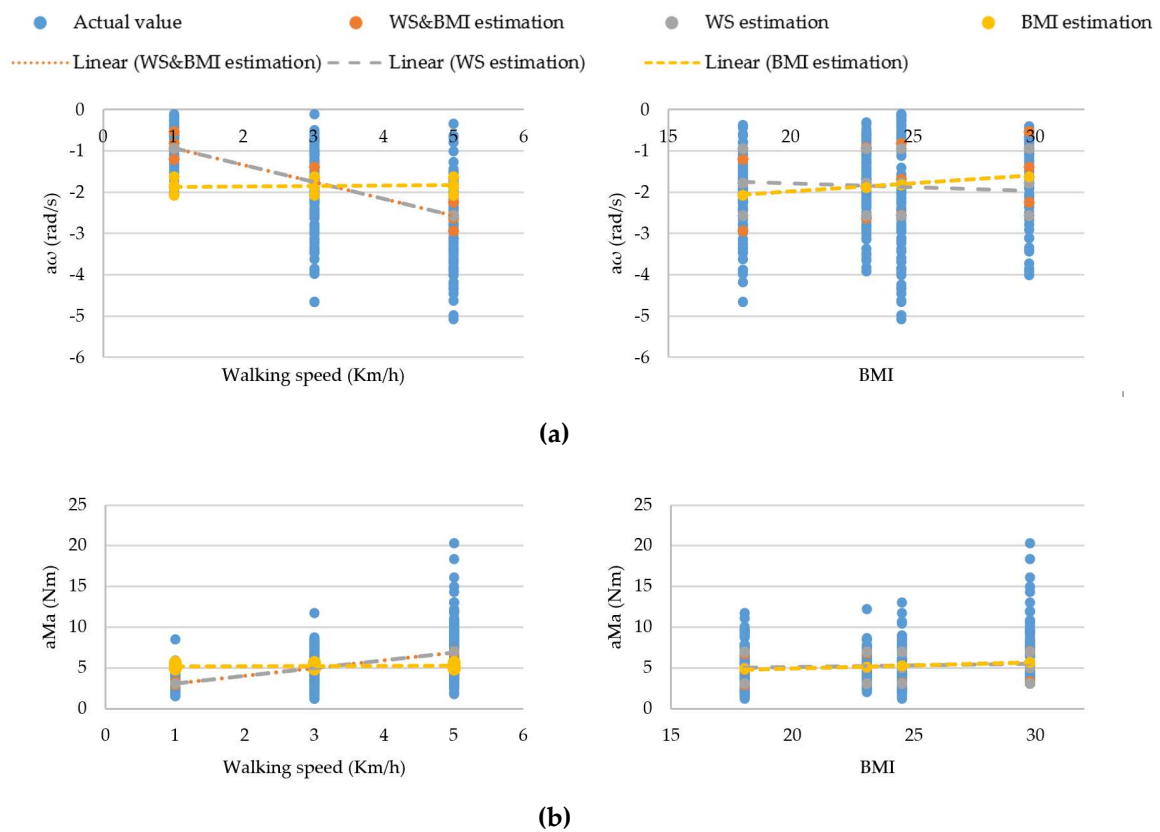


Figure 7. The regression of (a) average ankle velocity ($a\omega$) and (b) average ankle torque (aM_a) with different critical parameter during IC to FF phase.

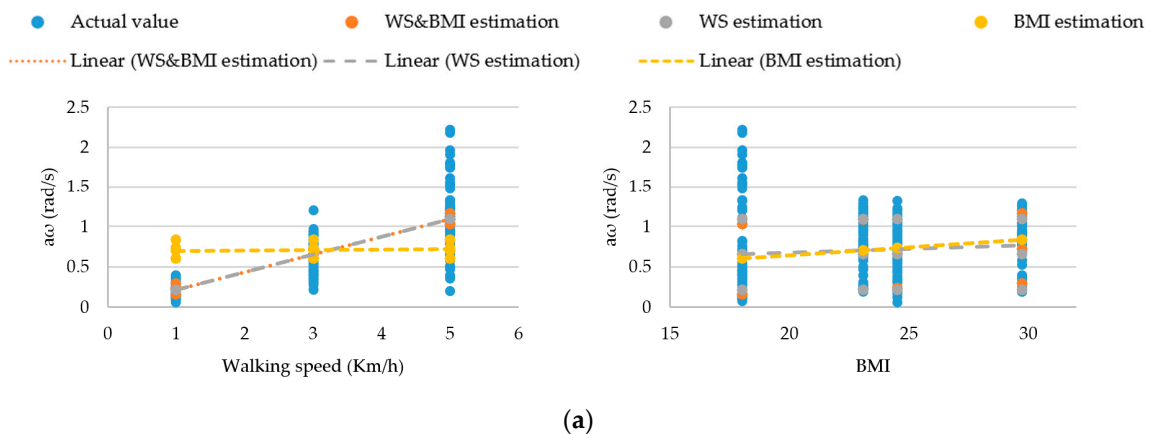


Figure 8. Cont.

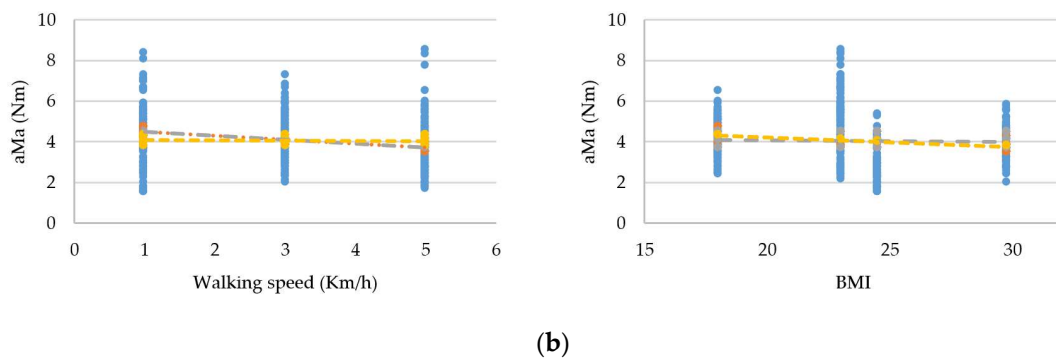


Figure 8. The regression of (a) average ankle velocity ($a\omega$) and (b) average ankle torque (aM_a) with different critical parameter during FF to HO phase.

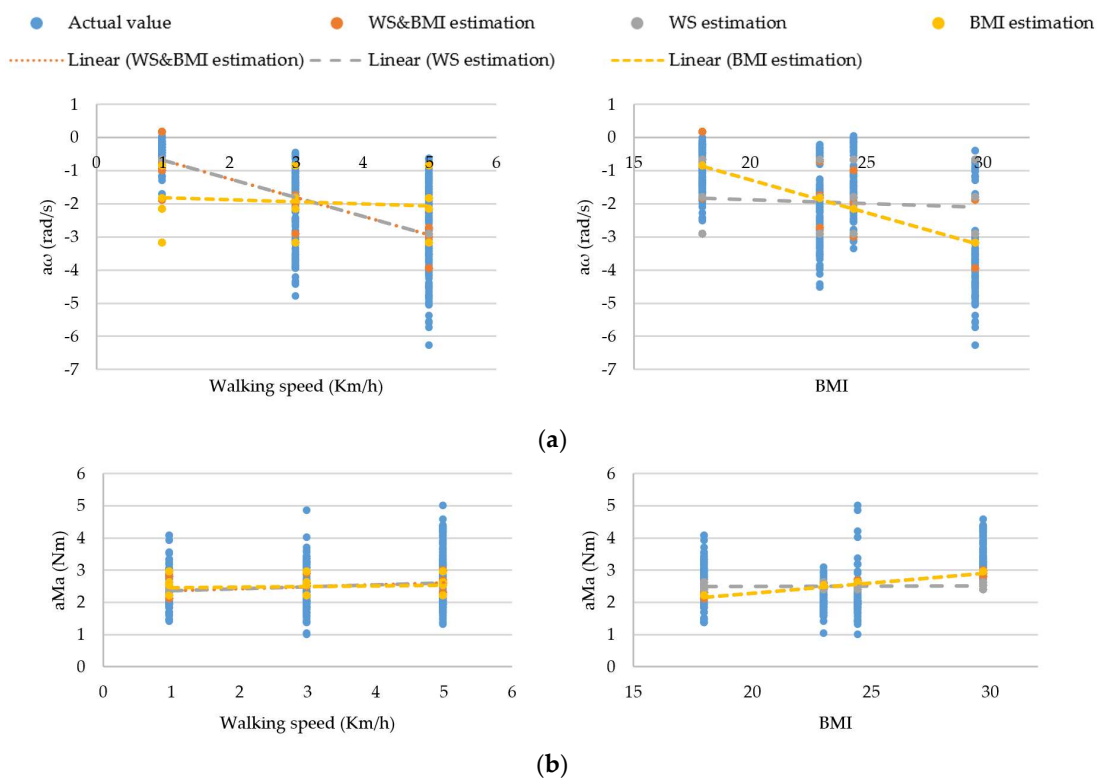


Figure 9. The regression of (a) average ankle velocity ($a\omega$) and (b) average ankle torque (aM_a) with different critical parameter during HO to TO phase.

Table 4. Regression statistic result.

Phase	Regression Statistics	$a\omega$			aM_a		
		WS	BMI	WS & BMI	WS	BMI	WS & BMI
IC to FF	Multiple R (p_1)	0.625	0.159	0.666	0.558	0.117	0.560
	R Square (p_1^2)	0.391	0.025	0.444	0.311	0.014	0.314
	Standard Error (Se1)	0.822	1.040	0.786	2.253	2.695	2.251
FF to HO	Multiple R (p_2)	0.830	0.199	0.837	0.246	0.154	0.277
	R Square (p_2^2)	0.689	0.039	0.700	0.060	0.024	0.077
	Standard Error (Se2)	0.235	0.413	0.231	1.245	1.270	1.236
HO to TO	Multiple R (p_3)	0.645	0.607	0.839	0.130	0.357	0.369
	R Square (p_3^2)	0.416	0.368	0.705	0.017	0.128	0.136
	Standard Error (Se3)	1.060	1.103	0.755	0.742	0.699	0.696
	Observations	480	480	480	480	480	480

The standard error (Se) results in Table 4 show that in general, the estimation of aM_a has higher Se compare to estimation of $a\omega$ ($Se1(aM_a) = 2.251 > Se1(a\omega) = 0.786$, $Se2(aM_a) = 1.236 > Se2(a\omega) = 0.231$, $Se3(aM_a) = 0.696 < Se3(a\omega) = 0.755$). BMI based estimation resulted in the highest estimated Se for each $a\omega$ and aM_a . On the other hand, the estimation based on walking speed only shows a smaller standard error, but the error reduced more when the two critical parameters were combined. For instance, during HO to TO, the standard error of $a\omega$ was 1.060 based on WS only, 1.103 based on BMI only, and 0.755 based on the combination of both. For illustrations of the reduced standard error, see Figures 7–9. The estimations based on both walking speed and BMI show wider coverage in hitting the actual value compare to estimation based on walking speed or BMI only.

The results of critical parameter coefficient estimation show that the WS coefficient consistently has the opposite sign between $a\omega$ and aM_a estimation for the whole stance phase, similar to the correlation analysis result. BMI coefficient results also show agreement with the correlation analysis result. The *t*-test results reveal that all coefficients for $a\omega$ estimation were significantly not possible to be zero (*P*-value < 0.05). However, some coefficient for aM_a estimation was insignificantly not possible to be zero. For instance, BMI coefficient has a confidence interval of -0.002 to 0.009 during IC to FF (*P*-value = 0.201), and WS coefficient has a confidence interval of 0.000 to 0.009 during HO to TO (*P*-value = 0.061).

Table 5. Critical parameter coefficient for multi regression of $a\omega$ and aM_a : estimation value and *t*-test result.

$a\omega$						
	Coefficients	Standard Error	Lower 95%	Upper 95%	t Stat	<i>P</i> -value
IC to FF						
Intercept	-1.807	0.234	-2.266	-1.347	-7.735	<0.05
WS	-0.431	0.025	-0.481	-0.380	-16.898	<0.05
BMI	0.058	0.010	0.039	0.077	6.035	<0.05
FF to HO						
Intercept	-0.238	0.069	-0.372	-0.103	-3.461	<0.05
WS	0.216	0.007	0.202	0.231	28.889	<0.05
BMI	0.011	0.003	0.005	0.016	3.740	<0.05
HO to TO						
Intercept	3.841	0.224	3.400	4.282	17.126	<0.05
WS	-0.508	0.024	-0.557	-0.460	-20.783	<0.05
BMI	-0.177	0.009	-0.195	-0.159	-19.244	<0.05
aM_a						
	Coefficients	Standard Error	Lower 95%	Upper 95%	t Stat	<i>P</i> -value
IC to FF						
Intercept	1.348	0.669	0.033	2.662	2.015	<0.05
WS	0.939	0.073	0.796	1.082	12.874	<0.05
BMI	0.035	0.003	-0.019	0.089	1.281	0.201
FF to HO						
Intercept	5.572	0.367	4.850	6.294	15.172	<0.05
WS	-0.187	0.040	-0.265	-0.108	-4.659	<0.05
BMI	-0.039	0.015	-0.068	-0.009	-2.565	<0.05
HO to TO						
Intercept	0.930	0.207	0.523	1.337	4.495	<0.05
WS	0.042	0.023	-0.002	0.087	1.881	0.061
BMI	0.061	0.008	0.045	0.078	7.225	<0.05

4. Discussion

The goal of this preliminary study was to identify whether ankle angular velocity or ankle torque is the better control reference parameter for implementation of stance assistance using MR brake in PICAFO. The control reference parameter must adapt to different subjects and walking

situations to maximize the benefit of using PICAFO [11]. Here, different subjects were represented by BMI, while the walking situations were represented by walking speed. Therefore, a superior control reference parameter is expected to have a high correlation with the BMI and walking speed during the stance phase.

The results of the regression analysis revealed that the ankle angular velocity is the preferable control reference parameter rather than ankle torque. The ankle angular velocity has a higher correlation score with BMI and walking speed compared to ankle torque, as shown in Table 3. The overall standard error of ankle angular velocity estimation is lower than the ankle torque estimation, which strengthens the correlation score result. The result of estimation and t-test of the critical parameter coefficient also shows the superiority of ankle angular velocity as control reference parameter where all the critical parameter coefficients were statistically significant not zero as shown in Table 4. However, the presented result cannot conclude the relationship between control reference and critical parameter due to a lack of sufficient participating subjects and regression model testing, which is a limitation of this study.

In the context of critical parameters, the results revealed that the combination of BMI and walking speed produced better estimations than a stand-alone parameter. Single-handedly, the walking speed alone already has enough correlation with both control reference parameters, especially ankle angular velocity, as shown in Table 3. This result agrees with the previous work by Kikuchi et al. in which the ankle angular velocity during IC to FF was predicted using the walking speed [32,33]. However, in this preliminary research, additional parameters such as BMI have been shown to improve the overall correlation score. Also, the standard error results support the correlation analysis. The standard error reduced when a combination of walking speed and BMI is used for estimation of ankle angular velocity, as shown in Table 3.

To sum up, the ankle angular velocity is the better choice for use as a control reference parameter, which can be estimated based on walking speed and BMI as revealed by the results. The implementation of the control reference parameter using the MR brake is also not difficult, because the feedback signal can be measured directly by using a rotary encoder. Ankle velocity can also be used to classify the gait phases [36]. This means that only rotary encoder is necessary as the sensor for both classification and control function in future implementation. Further study should be conducted in the future, which mainly focused on reducing the standard error of the control reference estimation. Improvement can be made by comparing a different kind of regression model and adding the sample sizes (subject number and walking speed). After obtaining a better fit estimation, the PICAFO system can implement the control reference parameter for stance assistance. Then, in a training session with the patient, for example, the therapist can optimally configure the PICAFO system simply by inserting the patient's walking speed and BMI.

Author Contributions: Conceptualization, D.A. and M.A.A.R.; methodology, N.N. and M.H.M.A.; formal analysis, D.A. and J.K.; investigation, D.A. and U.; resources, M.A.A.R, U. and S.A.M.; data curation, D.A. and M.K.S.; writing—original draft preparation, D.A.; writing—review and editing, D.A., M.A.A.R., U., N.N. and M.K.S.; supervision, M.A.A.R., U., S.A.M., and J.K.; funding acquisition, M.A.A.R. and U.

Funding: This research was funded by the Ministry of Education Malaysia, grant number 06G16 and the APC was funded by Malaysia Japan International Institute of Technology, Universiti Teknologi Malaysia. Some of the hardware was financially supported by Universitas Sebelas Maret (UNS) through Hibah Kolaborasi Internasional 2020 as well as partial funding from USAID through the Sustainable Higher Education Research Alliances (SHERA) Program, NCSTT with Contract No. IIE0000078-ITB-1.

Acknowledgments: The authors would like to express their appreciation to the Ministry of Education Malaysia, Universiti Teknologi Malaysia, Universitas Sebelas Maret, National Center for Sustainable Transportation Technology, and Institut Teknologi Telkom Surabaya for their financial support in this research.

Conflicts of Interest: The authors declare no conflict of interest.

References

1. BurrIDGE, J.; Taylor, P.; Hagan, S.; Swain, I. Experience of clinical use of the Odstock dropped foot stimulator. *Artif. Organs* **1997**, *21*, 254–260. [[CrossRef](#)] [[PubMed](#)]
2. Huo, W.; Mohammed, S.; Moreno, J.C.; Amirat, Y. Lower limb wearable robots for assistance and rehabilitation: A state of the art. *IEEE Syst. J.* **2016**, *10*, 1068–1081. [[CrossRef](#)]
3. Alam, M.; Choudhury, I.A.; Mamat, A.B. Mechanism and design analysis of articulated ankle foot orthoses for drop-foot. *Sci. World J.* **2014**, *2014*. [[CrossRef](#)] [[PubMed](#)]
4. Roche, N.; Bonnyaud, C.; Geiger, M.; Bussel, B.; Bensmail, D. Relationship between hip flexion and ankle dorsiflexion during swing phase in chronic stroke patients. *Clin. Biomech.* **2015**, *30*, 219–225. [[CrossRef](#)]
5. Chisholm, A.E.; Perry, S.D.; McLroy, W.E. Correlations between ankle-foot impairments and dropped foot gait deviations among stroke survivors. *Clin. Biomech.* **2013**, *28*, 1049–1054. [[CrossRef](#)]
6. Tanida, S.; Kikuchi, T.; Kakehashi, T.; Otsuki, K.; Ozawa, T.; Fujikawa, T.; Yasuda, T.; Furusho, J.; Morimoto, S.; Hashimoto, Y. Intelligently controllable Ankle Foot Orthosis (I-AFO) and its application for a patient of Guillain-Barre syndrome. In Proceedings of the 2009 IEEE International Conference on Rehabilitation Robotics, Kyoto, Japan, 23–26 June 2009; pp. 857–862.
7. Mahon, C.E.; Farris, D.J.; Sawicki, G.S.; Lewek, M.D. Individual limb mechanical analysis of gait following stroke. *J. Biomech.* **2015**, *48*, 984–989. [[CrossRef](#)]
8. Collins, S.H.; Bruce Wiggin, M.; Sawicki, G.S. Reducing the energy cost of human walking using an unpowered exoskeleton. *Nature* **2015**, *522*, 212–215. [[CrossRef](#)]
9. Mickelborough, J.; van der Linden, M.L.; Tallis, R.C.; Ennos, A.R. Muscle activity during gait initiation in normal elderly people. *Gait Posture* **2004**, *19*, 50–57. [[CrossRef](#)]
10. Mishra, A.K.; Srivastava, A.; Tewari, R.P.; Mathur, R. EMG analysis of lower limb muscles for developing robotic exoskeleton orthotic device. *Procedia Eng.* **2012**, *41*, 32–36. [[CrossRef](#)]
11. Adiputra, D.; Nazmi, N.; Bahiuddin, I.; Ubaidillah, U.; Imaduddin, F.; Rahman, M.A.; Mazlan, S.A.; Zamzuri, H. A review on the control of the mechanical properties of ankle foot orthosis for gait assistance. *Actuators* **2019**, *8*, 10. [[CrossRef](#)]
12. Delafontaine, A.; Gagey, O.; Colnaghi, S.; Do, M.-C.; Honeine, J.-L. Rigid ankle foot orthosis deteriorates mediolateral balance control and vertical braking during gait initiation. *Front. Hum. Neurosci.* **2017**, *11*, 214. [[CrossRef](#)] [[PubMed](#)]
13. Bregman, D.J.J.; de Groot, V.; van Diggele, P.; Meulman, H.; Houdijk, H.; Harlaar, J. Polypropylene ankle foot orthoses to overcome drop-foot gait in central neurological patients: A mechanical and functional evaluation. *Prosthet. Orthot. Int.* **2010**, *34*, 293–304. [[CrossRef](#)] [[PubMed](#)]
14. Tavernese, E.; Petrarca, M.; Rosellini, G.; Stanislao, E.D.; Pisano, A.; Rosa, G.D.; Castelli, E. Carbon Modular Orthosis (Ca.M.O.): An innovative hybrid modular ankle-foot orthosis to tune the variable rehabilitation needs in hemiplegic cerebral palsy. *Neurorehabilitation* **2017**, *40*, 447–457. [[CrossRef](#)] [[PubMed](#)]
15. Schrank, E.S.; Hitch, L.; Wallace, K.; Moore, R.; Stanhope, S.J. Assessment of a virtual functional prototyping process for the rapid manufacture of passive-dynamic ankle-foot orthoses. *J. Biomech. Eng.* **2013**, *135*, 101011. [[CrossRef](#)] [[PubMed](#)]
16. Frascarelli, F.; Masia, L.; Rosa, G.D.; Cappa, P.; Petrarca, M.; Castelli, E.; Krebs, H.I. The impact of robotic rehabilitation in children with acquired or congenital movement disorders. *Eur. J. Phys. Rehabil. Med.* **2009**, *45*, 135–141.
17. Adiputra, D.; Mazlan, S.U.; Zamzuri, H.; Rahman, M.A. Fuzzy logic control for ankle foot equipped with magnetorheological brake. *J. Teknol.* **2016**, *11*, 25–32. [[CrossRef](#)]
18. Adiputra, D.; Rahman, M.A.A.; Tjahjana, D.D.D.P.U.; Widodo, P.J.; Imaduddin, F. Controller development of a passive control ankle foot orthosis. In Proceedings of the International Conference on Robotics, Automation and Sciences, Melaka, Malaysia, 27–29 November 2017. [[CrossRef](#)]
19. Adiputra, D.; Mazlan, S.A.; Zamzuri, H.; Rahman, M.A.A. Development of controller for Passive Control Ankle Foot Orthoses (PICAFO) based on Electromyography (EMG) signal and angle. In Proceedings of the Joint International Conference on Electric Vehicular Technology and Industrial, Mechanical, Electrical, and Chemical Engineering (ICEVT & IMECE), Surakarta, Indonesia, 4–5 November 2015; pp. 200–206.
20. Nazmi, N.; Rahman, M.A.; Yamamoto, S.-I.; Ahmad, S.; Zamzuri, H.; Mazlan, S. A review of classification techniques of EMG signals during isotonic and isometric contractions. *Sensors* **2016**, *16*, 1304. [[CrossRef](#)]

21. Nazmi, N.; Rahman, M.A.A.; Yamamoto, S.I.; Ahmad, S.A. Walking gait event detection based on electromyography signals using artificial neural network. *Biomed. Signal Process. Control* **2019**, *47*, 334–343. [[CrossRef](#)]
22. Holgate, M.A.; Böhler, A.W.; Sugar, T.G. Control algorithms for ankle robots: A reflection on the state-of-the-art and presentation of two novel algorithms. In Proceedings of the 2nd Biennial IEEE/RAS-EMBS International Conference on Biomedical Robotics and Biomechatronics, Scottsdale, AZ, USA, 19–22 October 2008; pp. 97–102.
23. Boehler, A.W.; Hollander, K.W.; Sugar, T.G.; Shin, D. Design, implementation and test results of a robust control method for a powered ankle foot orthosis (AFO). In Proceedings of the IEEE International Conference on Robotics and Automation, Pasadena, CA, USA, 19–23 May 2008; pp. 2025–2030.
24. Blaya, J.A.; Herr, H. Adaptive control of a variable-impedance ankle-foot orthosis to assist drop-foot gait. *IEEE Trans. Neural Syst. Rehabil. Eng.* **2004**, *12*, 24–31. [[CrossRef](#)]
25. Chen, B.; Zhao, X.; Ma, H.; Qin, L.; Liao, W.-H. Design and characterization of a magnetorheological series elastic actuator for a lower extremity exoskeleton. *Smart Mater. Struct.* **2017**, *26*, 105008. [[CrossRef](#)]
26. Gordon, K.E.; Sawicki, G.S.; Ferris, D.P. Mechanical performance of artificial pneumatic muscles to power an ankle-foot orthosis. *J. Biomech.* **2006**, *39*, 1832–1841. [[CrossRef](#)] [[PubMed](#)]
27. Gordon, K.E.; Ferris, D.P. Learning to walk with a robotic ankle exoskeleton. *J. Biomech.* **2007**, *40*, 2636–2644. [[CrossRef](#)] [[PubMed](#)]
28. Fleischer, C.; Hommel, G. EMG-driven human model for orthosis control. In *Human Interaction with Machines Workshop*; Springer: Dordrecht, The Netherlands, 2006; pp. 69–76.
29. Emmens, A.R.; van Asseldonk, E.H.F.; van der Kooij, H. Effects of a powered ankle-foot orthosis on perturbed standing balance. *J. Neuroeng. Rehabil.* **2018**, *15*, 50. [[CrossRef](#)]
30. Kikuchi, T.; Tanida, S.; Otsuki, K.; Yasuda, T.; Furusho, J. Development of third-generation intelligently controllable ankle-foot orthosis with compact MR fluid brake. In Proceedings of the IEEE International Conference on Robotics and Automation, Anchorage, AK, USA, 3–7 May 2010; pp. 2209–2214.
31. Jiménez-Fabián, R.; Verlinden, O. Review of control algorithms for robotic ankle systems in lower-limb orthoses, prostheses, and exoskeletons. *Med Eng. Phys.* **2012**, *34*, 397–408. [[CrossRef](#)]
32. Kikuchi, T.; Tanida, S.; Yasuda, T.; Fujikawa, T. Automatic adjustment of initial drop speed of foot for intelligently controllable ankle foot orthosis. In Proceedings of the 2013 6th IEEE/SICE International Symposium on System Integration, Kobe, Japan, 15–17 December 2013; pp. 276–281.
33. Naito, H.; Akazawa, Y.; Tagaya, K.; Matsumoto, T.; Tanaka, M. An ankle-foot orthosis with a variable-resistance ankle joint using a magnetorheological-fluid rotary damper. *J. Biomech. Sci. Eng.* **2009**, *4*, 182–191. [[CrossRef](#)]
34. Guanzioli, E.; Cazzaniga, M.; Colombo, L.; Basilico, S.; Legnani, G.; Molteni, F. Assistive powered exoskeleton for complete spinal cord injury: Correlations between walking ability and exoskeleton control. *Eur. J. Phys. Rehabil. Med.* **2019**, *55*, 209–216. [[CrossRef](#)]
35. Winter, D.A. *Biomechanics and Motor Control of Human Movement*; John Wiley & Sons: Hoboken, NJ, USA, 2009. [[CrossRef](#)]
36. Grimmer, M.; Schmidt, K.; Duarte, J.E.; Neuner, L.; Koginov, G.; Riener, R. Stance and swing detection based on the angular velocity of lower limb segments during walking. *Front. Neurobot.* **2019**, *13*, 57. [[CrossRef](#)]

